A Top of Descent Prediction Model for Interaction-free Continuous Descent Operations

Chunyao Ma*, Debosmit Mookherjee*, Gabriel Mesquida-Masana†, Ramon Dalmau‡, Sameer Alam*
*Air Traffic Management Research Institute, Nanyang Technological University, Singapore
‡European Green Sky Directorate, EUROCONTROL Innovation Hub (EIH), Brétigny-Sur-Orge, France
†Thales Airspace Mobility Solutions, Singapore

***Abstract*—When air traffic controllers select the Top of Descent (TOD) location for flights without considering downstream traffic interactions, the descent process may get interrupted with level-offs to avoid conflicts. To support green aviation practices such as Continuous Descent Operations (CDO), this paper proposes a two-step learning model to predict TOD locations that lead to interaction-free descent trajectories to enable continuous descents. The first step involves identifying and learning from non-CDO flights whose descents were interrupted due to flight interactions. This process models the critical areas—primary zones containing interacting flights that may disrupt flight descents. In the second step, the model learns from CDO flights that have successfully maintained CDO notwithstanding the presence of potential interacting flights in the critical areas that cross paths or converge with the flight. A random forest-based model is trained to understand how the relationships between focal and potential interacting flights (e.g., relative altitudes, distances, convergence points) influence TOD decisions. TOD prediction results on the major arrival flow in Singapore flight information region (FIR), using the Air Traffic Management System (ATMS) data for November 2019, show that above 88% of the predicted TOD locations are within ±10nm of the actual TOD of the CDO flights on the test dataset, with a Mean Absolute Error of 5.14 nm. Moreover, testing the model on non-CDO flights with leveling-offs caused by flight interactions demonstrates that the prediction model can help avoid flight's leveling-offs by recommending a later TOD, allowing interacting flights to pass before the descent begins.**

***Index Terms*—Green Aviation; Continuous Descent Operations; Top of Descent; Machine Learning; Decision Trees; Random Forest.**

I. Introduction

Air transportation has experienced steady growth over recent decades, leading to increased demand and congestion in Terminal Maneuvering Areas (TMAs). This congestion contributes to increased holdings and Pilot-ATC communication, additional fuel consumption and greater environmental impact, along with rising operational costs. To address these challenges, Continuous Descent Operations (CDOs) have been implemented as a strategy to reduce fuel usage and mitigate associated environmental and economic impacts [1]. CDOs minimize intermediate level-offs, enabling aircraft to spend more time at higher, fuel-efficient altitudes [2]. However, their implementation faces challenges due to the complex and unpredictable nature of air traffic. This has driven research into optimizing procedure design, flight sequencing, and descent path planning to reduce unpredictability and enhance the overall effectiveness of CDOs [3].

In the literature, the most widely used approach for CDO implementation is the optimization of flight paths and schedules to maintain safe sequencing and spacing between flights. This includes strategies such as sequencing arrival aircraft and generating conflict-free trajectories through path-stretching techniques [4], computing dynamic arrival routes and times in predefined areas around the airport through 4D trajectory negotiation between Air Traffic Control (ATC) and pilots [5], and optimizing arrival routes to ensure temporal separation of all aircraft arriving at a TMA based on wake turbulence categories [6].

While meticulous planning of CDOs is crucial, it is essential to acknowledge that no plan is immune to uncertainty. Unforeseen factors, such as conflicts with departure or arrival traffic, may necessitate ATC interventions, including vectoring during the descent [7]. These interventions can significantly disrupt the pre-optimized descent profile, making it counterproductive to enforce CDOs for all flights with optimal planning. This is especially true during peak hours in major TMAs, where both efficiency and safety could be compromised [8]. Thus, implementing theoretically optimized descent schedules and arrival routes is challenging due to uncertainties.

CDO is often described as "the art of the possible", but is it feasible to maximize CDOs in current practices without meticulous planning? The answer could be yes. For aircraft cruising at typical altitudes of 30,000 to 40,000 feet (ft), the descent usually begins 100 to 130 nautical miles (nm) from the destination airport and can take up to 40 minutes before landing [9]. Given this long horizon, ATC and pilots are sometimes unaware of CDO opportunities due to limited visibility of downstream traffic [10]. The vertical descent profile is highly dependent on the choice of the Top of Descent (TOD) locations [11]. When a TOD is selected without considering downstream traffic and airspace conditions, it may result in the cancellation of CDOs to resolve conflicts with other flights. This situation underscores the need for predicting an optimal TOD location, taking into account potential interacting flights, to help minimize leveling-offs.

This paper proposes a TOD prediction model for interaction-free Continuous Descent Operations. First, an algorithm, based on EUROCONTROL criteria [12], is developed to distinguish between CDO and non-CDO flights and to identify TOD locations. In a second step, the upper and lower bounds of feasible TOD locations for CDO are determined

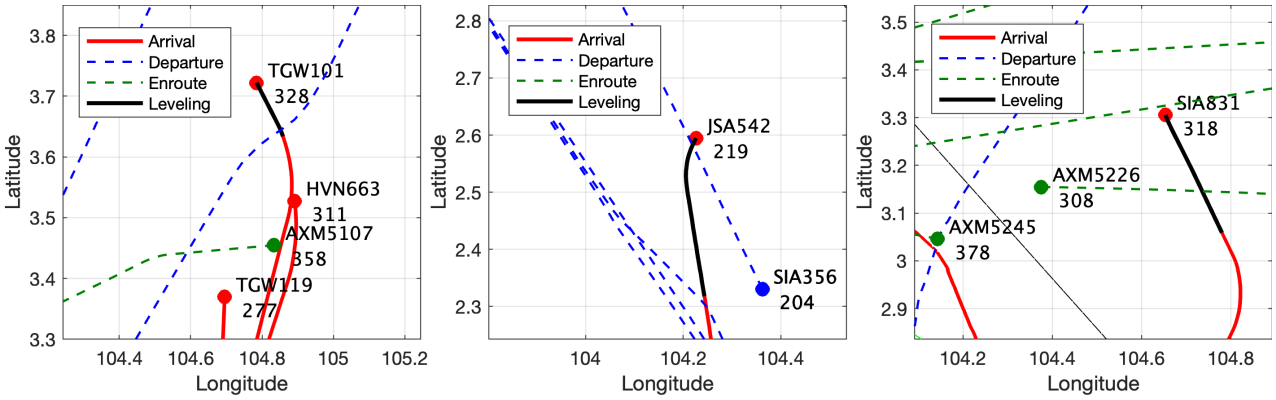

Figure 1. Examples of flight interactions causing leveling-offs.

using a linear fit of the distance to destination against the cruise altitude in historical data. When a flight enters its TOD upper bound, the flight features, the potential interacting flights, and the airspace conditions, such as holding patterns, demand, and runway configuration, are extracted for TOD prediction. To facilitate this, in the third step, critical areas containing potential interacting flights that can disrupt CDOs are modeled from level segments in non-CDO trajectories caused by encounters with other traffic. Flights within these critical areas that cross paths or converge with the focal flight are identified as potential interacting flights. Finally, a random forest-based interaction-free TOD prediction model is constructed to learn the relationships between the above features of successful CDO flights and their TOD locations.

II. Background

A. All flights can perform CDO, so why is it getting canceled mid-way?

The in-flight Flight Management System (FMS) provides both horizontal and vertical flight path guidance by considering real-time environmental inputs such as waypoints, airspace constraints, and wind forecasts [13]. Theoretically, a flight can achieve optimal CDO by following the FMS guidance, which optimizes speed and altitude to enhance fuel efficiency. However, the planned optimal CDO path suggested by the FMS is often overridden by pilots or ATC as the FMS solution does not account for scenarios involving multiple flights with complex interactions, making it impractical in such dynamic environments.

During descent, conflicts can arise between a flight and other arrival traffic at metering waypoints, or with departing and en-route flights when their lateral and vertical paths intersect. To maintain safe separation between aircraft, altitude adjustments may be issued, disrupting the CDO. Therefore, potential interactions with other flights must be carefully considered in advance of the descent to perform CDO effectively under complex traffic conditions.

B. Can the leveling-offs due to flight interactions be avoided?

As mentioned earlier, the TOD location significantly impacts the vertical descent path, which in turn influences future flight interactions that may lead to CDO disruption. Therefore, selecting the right TOD contributes to the avoidance of potential conflicting situations. This concept is supported by observations from real traffic scenarios. As shown in Fig. 1, the red solid lines, blue dashed lines, and green dashed lines in the three panels represent the lateral paths of arrival, departure, and en-route traffic within the Singapore FIR, respectively. The red, blue, and green dots indicate the locations of the corresponding flights at the moment captured in the traffic scenarios. Black solid lines mark the level segments on the descent paths. The three panels illustrate leveling-offs caused by interactions with arrival, departure, and en-route traffic, respectively. The numbers below the flight callsigns indicate flight altitude (in hundreds of feet). From the figure, it can be observed that if the three flights "TWG101," "JSA542," and "SIA831" had better management of TOD, there might have been sufficient vertical separation when they were laterally close to the encounter flights "HVN663," "SIA356," and "AXM5226.". Hence, the leveling-off could potentially have been avoided.

Current TOD prediction studies primarily focus on predicting the actual TOD location, regardless of whether the flights are CDO or non-CDO, of flights in historical data [14], often with a prediction error exceeding 30 nm, or on predicting TOD locations for idle-thrust descents [15]. However, none of these studies consider flight interactions, making them unsuitable for real-world traffic scenarios with complex interactions. Therefore, it is important to design a model that predicts TOD locations by taking into account potential interactions with other flights. Features that represent the relationships between the focal flight and nearby flights (e.g., relative altitudes, distances, convergence points) should be included to help the model understand how interactions influence TOD decisions.

III. Methodology

A. Methodology Overview

The concept diagram of the proposed two-step learning model for predicting TOD locations for interaction-free CDOs is illustrated in Fig. 2. The initial step focuses on analyzing non-CDO flights whose descents were interrupted by flight interactions and identifying the flights causing these disruptions.

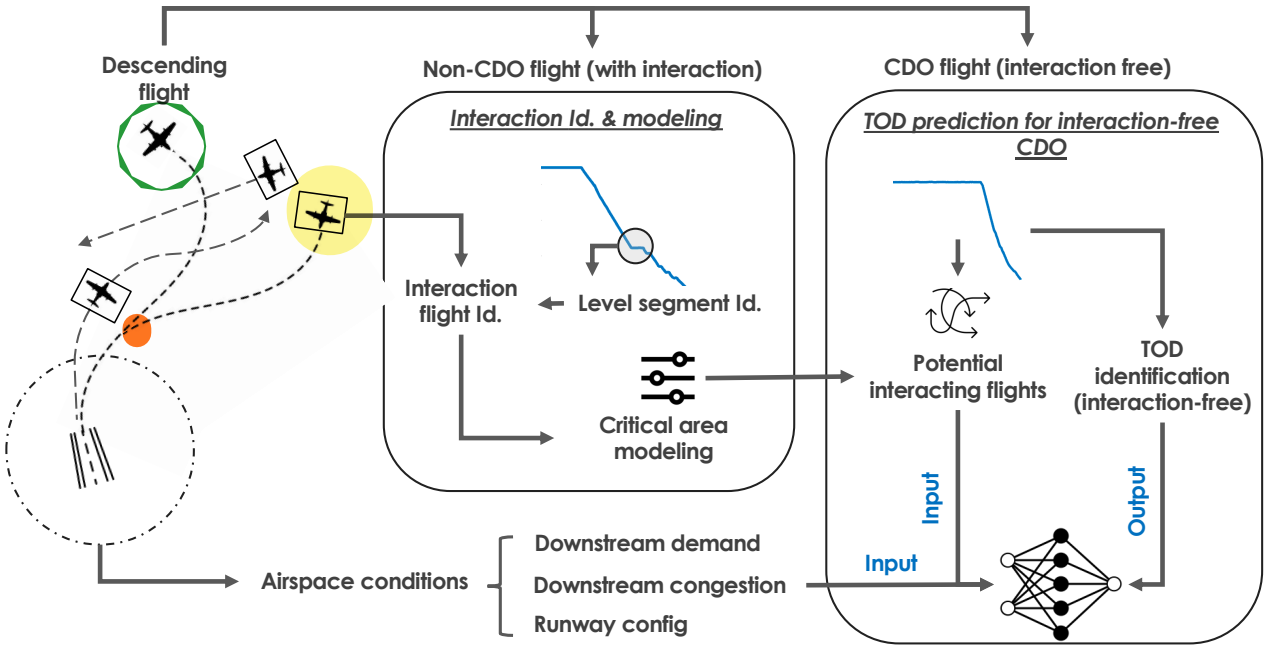

Figure 2. Concept diagram of the proposed TOD prediction model for interaction-free continuous descent operations.

This step involves modeling critical areas—key zones where interacting flights are likely to disturb descents for flights.

The second step involves analyzing flights that have successfully executed a CDO in spite of the presence of potential interacting flights within the critical areas. To identify the impact of the relationships between the focal flight and potential interacting flights (such as relative altitudes, distances, and convergence points) on TOD selection, this paper trains a random forest regressor. It operates by constructing multiple decision trees during training, each based on random subsets of the data and features, and combines their predictions through majority voting. This ensemble method reduces overfitting and improves accuracy compared to individual decision trees. It is robust, can handle missing data, and provides insights into feature importance.

B. CDO and TOD Identification

As mentioned earlier, the TOD is the point where an aircraft initiates its descent to a lower level in preparation for arrival at the destination airfield. In this paper, CDO flights are identified as those whose descent trajectories contain no level segments. Algorithm 1 outlines the steps for identifying the TOD locations of flights and determining whether their descent is classified as CDO or not, by using aircraft trajectory data and definitions provided by EUROCONTROL [12].

The algorithm iterates over the trajectory data, represented by latitude (ϕ), longitude (λ), altitude (h), and time (t), once the aircraft enters a 200 nautical mile radius of the destination airport. The first point where the aircraft initiates a descent is selected as the candidate TOD, and the cruising altitude at this point is set as the reference altitude. In order to avoid considering level segments that happen slightly below the reference altitude, the algorithm then checks if the flight maintains at least 90% of this reference altitude for a minimum duration of 5 minutes. If this condition is met, the end of this level segment is designated as the TOD. This adjustment is made to exclude level segments that may result from optimizing the cruising altitude based on the aircraft's weight, which should not be considered inefficient. If the above condition is not met, the initially identified candidate TOD is set as the TOD.

Algorithm 1 TOD and CDO Identification.

Require: Trajectory (ϕ, λ, h, t), Airport (AP), Distance to AP (d)
Ensure: TOD, CDO
TOD $\leftarrow \varnothing$, CDO $\leftarrow$ True, $h_{\text{ref}} \leftarrow \varnothing$
for each t where $d(t) \leq 200$ NM **do**
  if TOD $= \varnothing$ and $dh/dt < 0$ **then**
    $h_{\text{ref}} \leftarrow h(t)$, TOD $\leftarrow t$
    if $h(t) \geq 0.9 \times h_{\text{ref}}$ for ≥ 5 min **then**
      TOD $\leftarrow t$
    end if
  else if TOD $\neq \varnothing$ and $\left|\frac{dh}{dt}\right| < 300$ fpm for ≥ 20 sec **then**
    CDO $\leftarrow$ False
  end if
end for
Output: TOD, CDO

After identifying the TOD, the algorithm evaluates the descent rate for the remaining portion of the trajectory. If the vertical descent rate remains below 300 feet per minute for more than 20 seconds at any point after the TOD, an inefficiency is detected and the flight is categorized as non-CDO due to the presence of additional level segments. Otherwise, the flight is considered to be following a CDO.

C. Upper and Lower Bounds Modeling for CDO-feasible TOD

To predict the interaction-free TOD, the prediction must be made before the flight begins its descent, allowing the predicted TOD to be utilized to plan the descent. Therefore, it is crucial to understand the upper bound of possible TOD locations that enable a flight to perform CDO and to predict the interaction-free TOD location as the flight enters this upper bound.

The TOD location in this study is represented by its lateral distance to the destination airport. The reason for this representation, rather than using the geographical coordinates, is that latitude and longitude represent fixed points that may not align with the flight's navigational route, potentially leading to inaccuracies in descent planning. Moreover, modern flights use FMS that calculate and display TOD based on distance to the destination.

According to the widely adopted 3° descent path angle used in both operations and research related to flight descent procedures, the TOD location, i.e., distance to the destination, follows a linear trend relative to the cruise altitude [16]. To determine the upper and lower bounds of feasible TOD locations for a flight, this paper uses linear regression to model the TOD location against the cruising altitude based on historical data. A 95% prediction confidence interval is then applied to account for uncertainties and variances in the TOD locations, establishing the upper and lower bounds. The linear regression equation for modeling the TOD location $\hat{Y}$ is:

$$\hat{Y} = w_1 \cdot X + w_0, \tag{1}$$

where X is the cruising altitude, and w_1, w_0 are the regression coefficients. The 95% prediction interval for $\hat{Y}$ is given by:

$$\hat{Y} \pm t_{\alpha/2,n-2} \cdot \mathrm{SE}_{\hat{Y}}, \tag{2}$$

where $t_{\alpha/2,n-2}$ is the critical value from the t-distribution for a 95% confidence level, $\mathrm{SE}_{\hat{Y}}$ is the standard error of the prediction. This interval provides the lower and upper bounds, ensuring that the true TOD distance is captured within this range with 95% confidence.

D. Modeling Critical Areas of Flight Interactions for Interrupted CDOs

To predict a TOD location for an interaction-free CDO, it is crucial to understand where potential interacting flights may be located in the airspace as a flight enters its TOD upper bound. These areas are identified as critical areas of high likelihood of flight interactions. The critical areas not fixed as they vary for flights with different TOD upper bounds. Flights with a farther TOD may interact with flights from a wider area due to their longer descent trajectory compared to flights with a TOD closer to the airport. Therefore, the critical areas are modeled in accordance with different TOD upper bounds. The following subsections detail the identification process for critical areas and potential interacting flights.

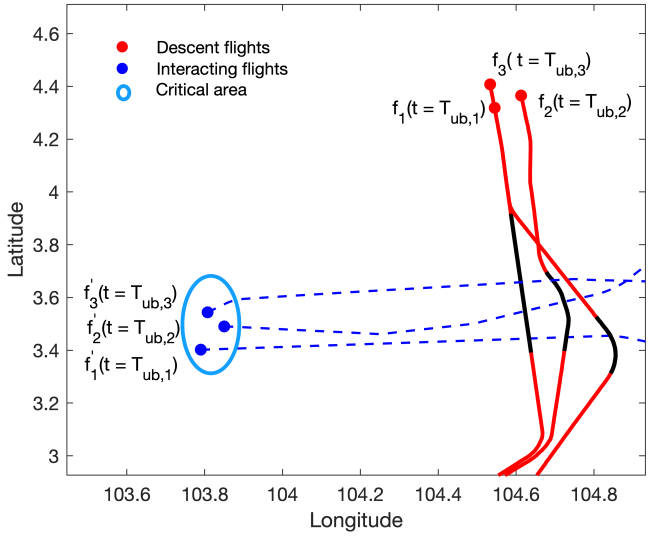

Figure 3. Critical area modeling. The critical areas are modeled by identifying the locations of flights (blue dots) that have caused level segments (black lines) in the descent trajectories at the moment the arrival flights (red dots) enter their TOD upper bounds.

1) Identification of Leveling-Offs Caused by Flight Interactions: The critical areas are modeled by identifying the flights that have caused leveled segments in the descent trajectories. Therefore, the first step is to determine whether a leveled segment in the descent path of a non-CDO flight is due to flight interactions. Therefore, the flight interactions in this paper focus on aircraft-to-aircraft encounters, where aircraft are in close proximity to each other and either aircraft could change its flight level or current path to avoid a potential conflict [17].

a) Interaction with cross-path flights: Interactions between a descending arrival flight and departing or en-route traffic primarily occur when their lateral flight paths intersect and they need to cross each other's altitude, increasing the likelihood of a loss of separation. In such cases, the descent process of the arriving flight is likely to be interrupted by maintaining a certain altitude until the conflicting situation is resolved, i.e., until lateral separation is ensured. Conflicting cross-path flights that lead to leveling-offs are identified as those with a potential loss of lateral separation at the start of the leveling-off and no conflict at the end of the leveling-off.

Denote the 4D trajectory of the focal arrival flight as $f_i(\phi_{t,i}, \lambda_{t,i}, h_{t,i}, t_i)$ and the cross-path flight as $f_i^{'}(\phi_{t,i}^{'}, \lambda_{t,i}^{'}, h_{t,i}^{'}, t_i^{'})$. Denote the distance between the two flights at the closest point of approach $d^*_{f_i,f_i^{'}}$ and the corresponding time as $t^*_{f_i,f_i^{'}}$. Denote the start time of the leveling-off of f_i as T_{s,f_i} and the end time as T_{e,f_i}. Therefore the interacting flight $f_i^{'}$ is identified as:

$$\begin{aligned} f_i^{'} \quad & \leftarrow fc_{j,i}(j = 1, 2, ..., N_{cross,i}) \\ \text{s.t.} \quad & d^*_{f_i,fc_{j,i}} \leq 5\text{nm} \\ & T_{s,f_i} \leq t^*_{f_i,fc_{j,i}} \leq T_{e,f_i}, \end{aligned} \tag{3}$$

where $fc_{j,i}$ represents the j^{th} cross-path flight of f_i, and $N_{cross,i}$ is the total number of cross-path flights.

b) Interaction with converging flights: Interactions between two arriving flights typically occur when the flights are consecutive in the arrival sequence or converging towards a metering fix to follow the Standard Terminal Arrival Routes (STARs) for sequencing before landing. Thus, the interactions between arrival flights are identified based on the following criteria:

$$\begin{aligned} f_i^{'} \quad & \leftarrow fa_{j,i}(j=1,2,...,N_{arv,i}) \\ \text{s.t.} \quad & d_{t,i}^{AP} \geq d_{t,fa_{j,i}}^{AP}, t=T_{e,f_i} \\ & d_{f_i,fa_{j,i}} \leq d_0, t=T_{e,f_i} \\ & h_{t,j}-h_{t,i} \leq 1000\text{ft}, t=T_{s,f_i} \\ & h_{t,j}-h_{t,i} > 1000\text{ft}, t=T_{e,f_i}, \end{aligned} \tag{4}$$

where $fa_{j,i}$ represents the j^{th} converge-path flight with f_i, and $N_{arv,i}$ is the total number of converge-path flights. d_0 is a lateral distance threshold to ensure the two flights are close enough to have interaction. In the experimental study of this paper, it is set as 15nm.

2) Critical Area Modeling: By identifying interacting flights, we can ascertain the locations of other aircraft when a non-CDO flight, potentially influenced by these interactions, enters the TOD upper boundary. As shown in Fig. 3, the TOD upper bound of f_1, f_2, and f_3, represented by red dots, is between 180nm to 190nm. When they enter their TOD upper bounds, the locations of their interacting flights, which later have caused the leveled segments indicated by the black lines, are depicted by blue dots. The area containing these interacting flights, marked by the blue ellipse, represents the modeled critical area of interactions for flights within this upper bound category. By modeling such critical areas for different upper bound categories, the primary zones containing interacting flights that may disrupt the flight's descent for flight with different TOD upper bounds are identified.

E. Airspace Condition Description

Besides accounting for potential interactions between flights and avoiding conflict situations, TOD prediction also requires a dynamic assessment of multiple factors.

The specific runways in use at the time of arrival can influence the TOD location. Different runways may require varying approach paths since different STARs are designated based on runway configurations, which often change due to factors such as wind direction and influences the TOD locations where descent should be initiated. Moreover, the number of available runways, whether designated separately for landings and departures or used interchangeably, affects the airport capacity and how incoming flights are being sequenced. In this paper, the runway usage is represented by the runways designated for landing and taking off:

$$Rwy_t = \begin{bmatrix} Dep_{1,t}, Dep_{2,t}, ..., Dep_{i,t}, ..., Dep_{N_{rwy},t} \\ Arv_{1,t}, Arv_{2,t}, ..., Arv_{i,t}, ..., Arv_{N_{rwy},t} \end{bmatrix}, \tag{5}$$

where $Dep_{i,t}(Arv_{i,t}) = 1$ if runway i is used for taking-off (landing) at time t, otherwise $Dep_{i,t}(Arv_{i,t}) = 0$.

Conditions in the terminal airspace, such as demand and congestion, can influence when an aircraft should begin its descent. For instance, during peak demand times, controllers may instruct flights to start their descent earlier to space out arrivals over a longer distance and time for landing procedures and preventing flights from experiencing go-arounds. Therefore, this paper takes into consideration the demand features $N50_{t,p}$, $N100_{t,p}$ at t, which represent the number of flights within a 50nm and 100nm radius of the destination airport during a time window of length p before t. The congestion (indicated by holdings in this paper) is depicted by $H50_{t,p}$, $H100_{t,p}$ at t. These values denote the number of flights caught in holding within a 50nm and 100nm radius of the destination airport during a time window of length p before t. To incorporate the temporal evolution of demand and congestion, there values in the previous time window are also considered, including $N50_{t-p,p}$, $N100_{t-p,p}$ $H50_{t-p,p}$, and $H100_{t-p,p}$.

F. Interaction-free TOD prediction

Flights within the critical areas that cross paths or converge with the flight f_i are considered as potential interacting flights. Features of its j^{th} interacting flight $f_{j,i}^{'}$ at t include altitude $h_{j,i,t}$, ground speed $v_{j,i,t}$, distance to the airport $d_{j,i,t}^{AP}$, distance to the converge/intersection point $d_{j,i,t}^{C}$, distance to the focal flight $d_{f_{j,i}^{'},f_i}$, and the distance of the focal flight to the intersection $d_{i,t}^{C}$.

Features of the interacting flights, together with the airspace condition features, and the characteristics of the focal flight constitute the input features for the TOD prediction model. Beside the altitude and geographical coordinates, the ground speed $v_{t,i}$, the upper bound ub_i and the lower bound lb_i of the feasible TOD range, and the aircraft type AC_i of f_i are considered. Thus, the full input of f_i can be represented as:

$$\mathbf{X}(i,t) = \begin{bmatrix} Rwy_t; \\ \phi_{t,i}, \lambda_{t,i}, h_{t,i}, v_{t,i}, ub_i, lb_i, AC_i; \\ f_{1,i}^{'}, f_{2,i}^{'}, ..., f_{j,i}^{'}, ..., f_{N_C,i}^{'}; \\ N50_{t,p}, N100_{t,p}, H50_{t,p}, H100_{t,p}; \\ N50_{t-p,p}, N100_{t-p,p}, H50_{t-p,p}, H100_{t-p,p}. \end{bmatrix} \tag{6}$$

where $t = T_{ub,i}$, i.e., when f_i enters its TOD upper bound.

The dataset X is comprised of both numerical and categorical features. Categorical features, such as *Aircraft type* and *runway configuration*, are transformed using label encoding. The mapping function, $f : Cat \rightarrow \mathbb{Z}$, assigns each category c_i to an integer $i-1$. The target variable $\mathbf{Y}$ represents the distance between the TOD and the destination airport. Sorted by the time of flights entering the FIR, the first 80% flights are used for training and the other 20% for testing.

The model selected for this study is a Random Forest regressor, an ensemble method well-suited for capturing complex, non-linear relationships. The random forest regressor $f(X)$ is an ensemble of T decision trees $\{f_t(X)\}_{t=1}^{T}$, where each tree is trained on a bootstrapped subset of the data. The output of

the forest is the average prediction of all trees. The training process of the random forest regressor can be represented as follows:

$$\hat{Y} = f(X) = \frac{1}{N_T} \sum_{t=1}^{T} \text{Tree}_t\left(X, \mathcal{D}_t\right) \tag{7}$$

where $\hat{Y}$ is the predicted value for X, N_T is the number of decision trees in the forest, $\text{Tree}_t\left(X, \mathcal{D}_t\right)$ is the prediction from the t-th decision tree, trained on a bootstrapped subset $\mathcal{D}_t$ of the training data, and $\mathcal{D}_t \subseteq \mathcal{D}$ is a randomly sampled subset (with replacement) of the training data.

To optimize the model, a randomized search was performed over a predefined hyperparameter grid. The parameter grid explored was:

$$\texttt{grid} = \begin{cases} n\_estimators : [50, 100, 200, 300, 400, 500, 1000] \\ max\_features : [\sqrt{p}, \log_2 p, \text{None}] \\ max\_depth : [\text{None}, 10, 20, 30, \ldots, 100] \\ min\_samples\_split : [2, 5, 10, 15] \\ min\_samples\_leaf : [1, 2, 4, 6] \\ bootstrap : [\text{TrueFalse}] \end{cases}$$

where p denotes the number of input features. The randomized search was conducted over 20 iterations, each sampling a different combination of hyperparameters. The model's performance was evaluated based on the criterion of minimizing the mean squared error (MSE):

$$\text{MSE} = \frac{1}{n} \sum_{i=1}^{n} \left(Y_i - \hat{Y}_i\right)^2$$

where y_i and $\hat{y}_i$ are the true and predicted values, respectively, and n represents the number of samples in the test set. The hyperparameter configuration resulting in the lowest MSE was chosen as the optimal model.

IV. Experimental Study

To verify the effectiveness of the proposed method for TOD prediction, we have carried out a case study based on the air traffic data during November 2019 in Singapore FIR to predict the TOD locations for CDO flights in one of the major arrival flows to Singapore Changi airport (WSSS).

The arrival traffic in Singapore TMA primarily originates from four directions: north, south, west, and east. Figure 4 illustrates a day's traffic within the Singapore FIR. The red lines represent the trajectories of the arrival flights in the selected major flow, referred to as the center PASPU flow in the remainder of this paper, while the blue lines are flights in other arrival flows. The gray lines depict the tracks of the departure flights from WSSS and en-route flights transiting through Singapore FIR. The black lines indicate the level segments during the flights' descent. It can be observed that most leveling offs occur at the intersections between the arrival flows and the departure or en-route flows, as well as around

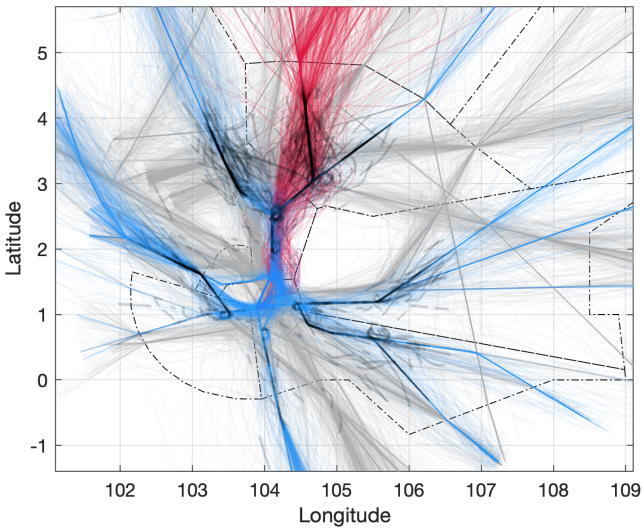

Figure 4. A snapshot of one day's traffic in Singapore FIR. Red lines represent the trajectories of arrival flights in the central PASPU flow , while blue lines show other arrival flows. Gray lines indicate the tracks of departure flights and en-route flights. Black lines highlight the level segments during the flights' descent.

the merge point of two or more arrival flows. This observation substantiates that flight interactions are the primary cause of leveling-offs during descent.

It can also be observed that three major flows converge into the descending traffic from the north direction of the TMA. The central PASPU flow experiences substantial interactions with departure, en-route, and other arrival traffic. This is evidenced by the highest number and density of level segments compared to other arrival flows in the FIR. Consequently, this paper focuses on predicting the TOD location for flights in the central PASPU flow . There are a total number of 1197 CDO flights and 1708 non-CDO flights in the central PASPU flow.

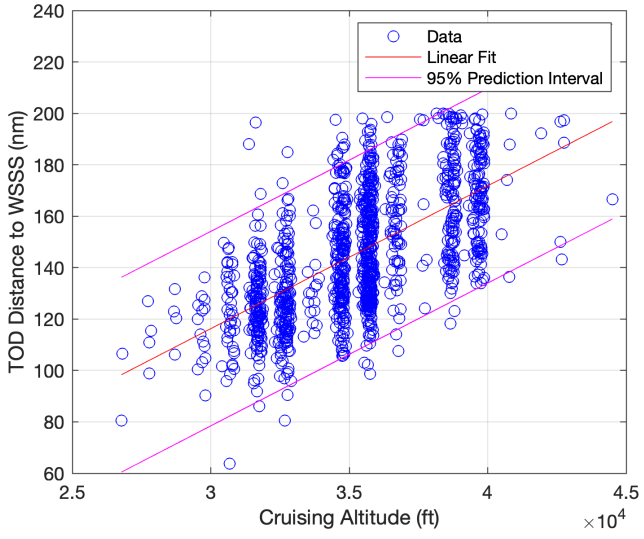

Figure 5. The identified upper and lower bounds, depicted by the pink lines, for CDO-feasible TODs based on the cruise altitude.

A. Upper and Lower Bound Modeling for CDO-feasible TOD

After identifying the TOD location for the arrival flights in the central PASPU flow and categorizing them into CDO and

non-CDO flights, the upper and lower bounds of the CDO-feasible TOD locations are modeled from the altitude and distance to WSSS airport of the CDO flights at their TOD. As shown in Fig. 5, the blue dots are the TOD locations, depicted by the distance from the TOD to the WSSS airport, versus the flights' cruise altitude. The distance to airport is generally assumed to follow a linear trend in accordance with the cruise altitude.

A linear regression, the red line, concludes that $y = 0.0056x - 50.3722$, and x and y here correspond to the data values at the x-axis and y-axis. The standard deviation of the fit is 19.2618nm. The pink lines show the 95% percent prediction interval of the linear fit. The upper line of the 95% prediction interval is determined as the upper bound of the TOD locations according to the flights' cruise altitude. To address potential concerns about data dispersion in Fig. 5, it's worth noting that while variability is present, the linear trend remains clear. The observed dispersion can result from various factors, including aircraft type, wind conditions, STARs, and speed variations. This variability does not significantly impact the prediction outcome as, at this step, we only intend to establish a boundary for TOD prediction process initiation. By defining this boundary, we ensure that the prediction is neither conducted too early, where accuracy might be compromised, nor too late, after the flight has already passed the optimal TOD location.

B. Critical Area Modeling for Different TOD Upper Bound Categories

When a flight enters its TOD upper bound, as calculated by its cruise altitude, the proposed TOD prediction model will make predictions based on flight interactions as well as airspace conditions. The critical areas containing potential interacting flights when a flight enters the TOD upper bound are presented in Fig. 6. The TOD upper bounds are divided into five categories: less than 160nm, 160nm to 170nm, 170nm to 180nm, 180nm to 190nm, and greater than 190nm. The blue dots in each panel represent the locations of the corresponding interacting flights at the moment that the descent flights in each category reached the location of their TOD upper bounds. As the upper bound extends, the critical area not only grows in size but also tends to shift farther away from the airport. This pattern arises because when a flight's TOD is located farther from the airport, the interacting flights during its descent are typically positioned farther out as well and are more sparsely distributed compared to those associated with a closer TOD.

C. TOD Prediction Model Training and Testing

When a flight enters its CDO boundary, the flights within the corresponding critical area are extracted. They include departure and en-route flights that potentially cross paths as well as arrival flights that converge with the focal flight. They are all identified as the potential interacting flights. Features of these selected flights and their relationships with the focal flight are used to characterize the interactions and predicting an interaction-free TOD. These features include altitude, speed,

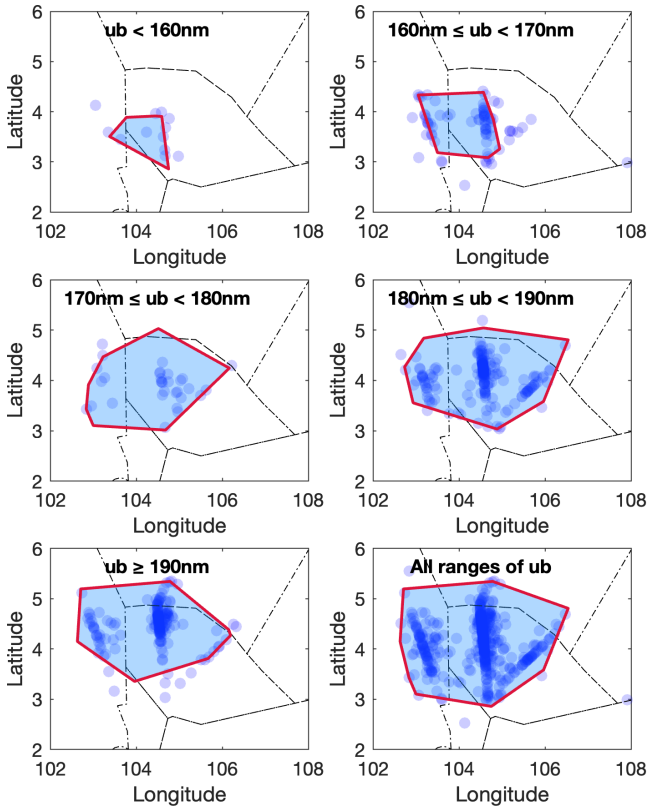

Figure 6. The critical areas containing interacting flights for different TOD upper bound categories.

distance to the airport, distance to the intersection, distance to the focal flight, and the distance of the focal flight to the intersection.

The training dataset contains 966 CDO flights, while the test dataset contains 231 CDO flights. The best parameters identified by the grid search are: $n\_estimators = 400$, $min\_samples\_split = 2$, $min\_samples\_leaf = 1$, $max\_features = sqrt$, $max\_depth = 20$, and $bootstrap = True$.

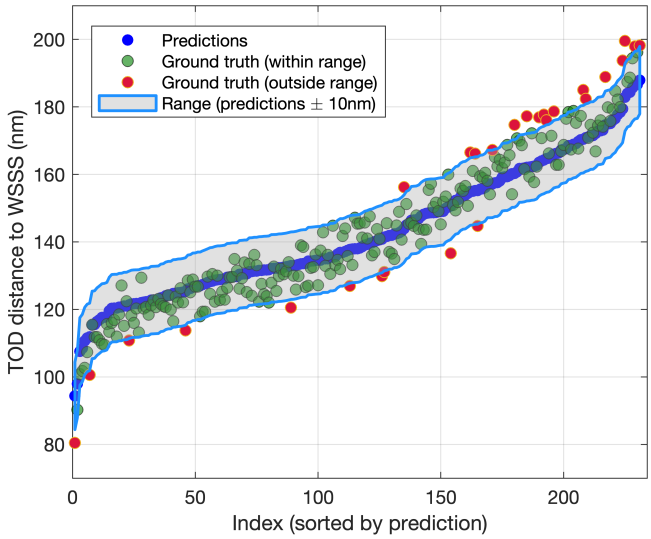

Figure 7. Comparison of the predicted TOD with the ground truth shows that 88.13% of the actual TOD fall within a $\pm 10nm$ range of the prediction.

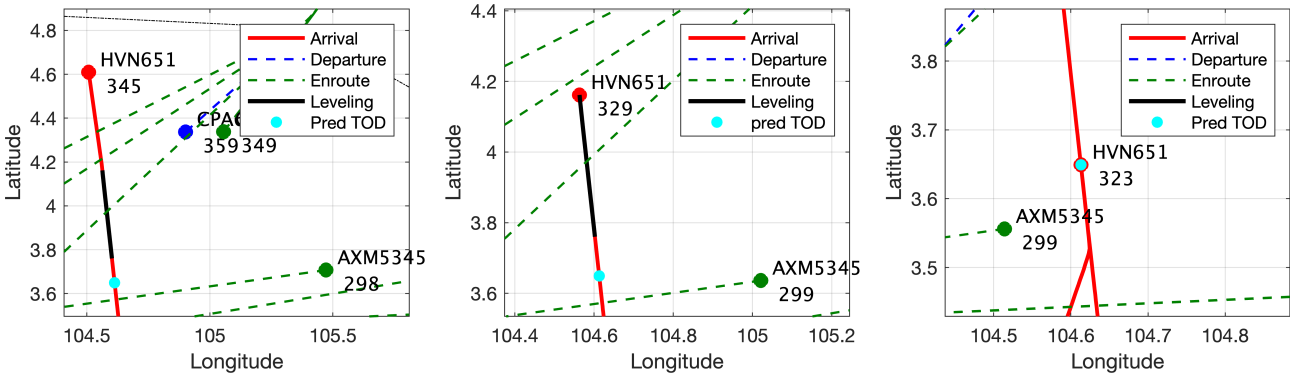

Figure 8. Application of the trained TOD prediction model on a non-CDO flight (HVN651). If HVN651 had initiated its descent at the predicted TOD location, marked by the cyan dot, the leveling-off could have been avoided as the interacting flight AXM5345 would have already passed the crossing point.

The Mean Squared Error (MSE), Root Mean Square Error (RMSE), Mean Absolute Error (MAE), and R-Squared on the training dataset are $35.103nm^2$, 5.925nm, 4.838nm, and 0.936, respectively. And their values on the testing dataset are $40.518nm^2$, 6.365nm, 5.143nm, and 0.926, respectively. This prediction results show that the mean distance between the predicted and the true interaction-free TOD location is 5.143nm. Compared with the result of existing TOD prediction models in [18] and [14] which predicted the actual TOD location without counting in flight interactions and have prediction errors above 30nm, the 5.143nm prediction error represents a significant improvement over these models.

Fig. 7 compares the predicted TOD location and the ground truth. The x-axis is the index of the flight in the test dataset, i.e., 1–231. The y-axis shows the TOD locations, i.e., the distance to WSSS at TOD. The blue dots represent the predicted value. The green dots and red dots represents the ground truth values that falls within and outside the $\pm$10nm range of the predicted values. It can be seen that the majority of the true values, which is 88.13%, are within this range.

Figure 8 demonstrates the application of the TOD prediction on a non-CDO flight (HVN651) whose leveling-off (indicated by the black solid line) was caused by interactions with another flight (AXM5345). The right panel displays the traffic situation at the TOD of HVN651. The distances of both flights to the point of interaction are similar, suggesting a likely future conflict. The middle panel illustrates the traffic at the start of the leveling-off, where the vertical separation between the two flights is 3,000 feet, indicating a potential loss of separation without the leveling-off maneuver. However, if HVN651 had initiated its descent at the predicted TOD location, marked by the cyan dot, the interaction could have been avoided as AXM5345 would have already passed the crossing point. Such scenarios are frequently observed in other non-CDO flights, highlighting the potential of the prediction model to enable interaction-free CDO operations.

V. Conclusions and Discussions

This paper presents a novel approach to predicting Top of Descent (TOD) locations to enable interaction-free Continuous Descent Operations (CDO).

The proposed model first analyzes non-CDO flights to identify critical areas—zones where interactions are likely to disrupt descent, and then learns from CDO flights that successfully maintained uninterrupted descents in spite of the presence of potential conflicts. By incorporating key features such as relative altitudes, distances, convergence points, and overall airspace conditions, the model captures the complex relationships between the focal flight and its interacting flights with a Mean Absolute Error (MAE) of 5.143nm compared with the true TOD locations for interaction-free CDO. Testing on non-CDO flights demonstrates that the predicted TODs can potentially avoid leveling-offs by recommending later TODs increasing separation to previously conflicting flights.

The proposed methodology and experimental results in this paper do have several limitations. A primary limitation is the absence of wind data, which is one of the most critical factors influencing TOD for flights. To improve the effectiveness of the TOD prediction model, future work should incorporate wind information. Another limitation is that the predicted TOD for achieving an interaction-free CDO is not thoroughly validated in this paper. Future research should focus on testing the validity of the predicted TOD, either through aircraft performance-based trajectory simulations or by generating trajectories from past air traffic data. Additionally, maintaining a continuous descent without leveling-offs may not always yield the greatest benefits in terms of fuel consumption and environmental impact. To provide a more comprehensive assessment, future studies could quantify the advantages of interaction-free TOD predictions using alternative metrics, such as fuel consumption and emission reductions.

Acknowledgment

This research is supported by the National Research Foundation, Singapore, and the Civil Aviation Authority of Singapore, under the Aviation Transformation Programme. Any opinions, findings and conclusions or recommendations expressed in this material are those of the author(s) and do not reflect the views of National Research Foundation, Singapore and the Civil Aviation Authority of Singapore.

References

[1] J. Rosenow, M. Lindner, and J. Scheiderer, "Advanced flight planning and the benefit of in-flight aircraft trajectory optimization," *Sustainability*, vol. 13-3, p. 1383, 2021.

[2] R. Dalmau Codina, J. Sun, and X. Prats Menéndez, "Fuel inefficiency characterisation and assessment due to early execution of top of descents. a case study for amsterdam-schiphol terminal airspace using ads-b data," in *14th USA/Europe ATM R&D Seminar (virtual event)*, 20-24 September, 2021.

[3] L. Yang, W. Li, S. Wang, and Z. Zhao, "Multi-attributes decision-making for CDO trajectory planning in a novel terminal airspace," *Sustainability*, vol. 13, no. 3, p. 1354, 2021.

[4] D. Gui, M. Le, Z. Huang, J. Zhang, and A. D'Ariano, "Optimal aircraft arrival scheduling with continuous descent operations in busy terminal maneuvering areas," *Journal of Air Transport Management*, vol. 107, p. 102344, 2023.

[5] S. Alam, M. Nguyen, H. Abbass, C. Lokan, M. Ellejmi, and S. Kirby, "Multi-aircraft dynamic continuous descent approach methodology for low-noise and emission guidance," *Journal of Aircraft*, vol. 48, no. 4, pp. 1225–1237, 2011.

[6] T. Polishchuk, V. Polishchuk, C. Schmidt, R. Sáez García, X. Prats Menéndez, H. Hardell, and L. Smetanová, "How to achieve CDOs for all aircraft: Automated separation in tmas-enabling flexible entry times and accounting for wake turbulence categories," in *10th SESAR Innovation Days, Virtual conference*, 7-10 Dec 2020.

[7] Y. Chen, Y. Zhao, and Y. Wu, "Recent progress in air traffic flow management: A review," *JATM*, vol. 116, p. 102573, 2024.

[8] ICAO, "Continuous Descent Operations (CDO) manual," *ICAO-Doc-9931, Montreal, QC, Canada*, 2010.

[9] E. A. Alharbi, L. L. Abdel-Malek, R. J. Milne, and A. M. Wali, "Analytical model for enhancing the adoptability of continuous descent approach at airports," *Applied Sciences*, vol. 12, no. 3, p. 1506, 2022.

[10] R. Dalmau and X. Prats, "Controlled time of arrival windows for already initiated energy-neutral continuous descent operations," *Transportation Research Part C: Emerging Technologies*, vol. 85, pp. 334–347, 2017.

[11] H. Aksoy, E. T. Turgut, and Ö. Usanmaz, "The design and analysis of optimal descent profiles using real flight data," *Transportation Research Part D: Transport and Environment*, vol. 100, p. 103028, 2021.

[12] Eurocontrol, "European action plan for continuous climb and descent operations," Eurocontrol, Tech. Rep., 2020.

[13] R. Collinson, "Autopilots and flight management systems," in *Introduction to Avionics Systems*. Springer, 2023, pp. 259–284.

[14] H. J. Ang, Q. Cai, and S. Alam, "A deep neural network approach for prediction of aircraft top of descent," in *Proc. of Itl. Workshop on ATM/CNS 2022*. ENRI, 25-27 Oct, 2022, Tokyo, Japan, pp. 208–215.

[15] L. Stell, "Prediction of top of descent location for idle-thrust descents," in *9th USA/Europe ATM R&D Seminar, Berlin, Germany*, June 14-17, 2011, pp. 1–10.

[16] M. Kanazaki, N. Setoguchi, and R. Saisyo, "Evolutionary algorithm applied to time-series landing flight path and control optimization of supersonic transport," *Neural Computing and Applications*, pp. 1–13, 2023.

[17] S. MORTON, "Eurocontrol specification for medium-term conflict detection, eurocontrol-spec-0139," Eurocontrol, Tech. Rep., 2017.

[18] T. Z. Y. Benjamin, S. Alam, and C. Y. Ma, "A machine learning approach for the prediction of top of descent," in *2021 IEEE/AIAA 40th Digital Avionics Systems Conference (DASC)*. IEEE, 25-28 Oct, 2021, Online, pp. 1–10.